



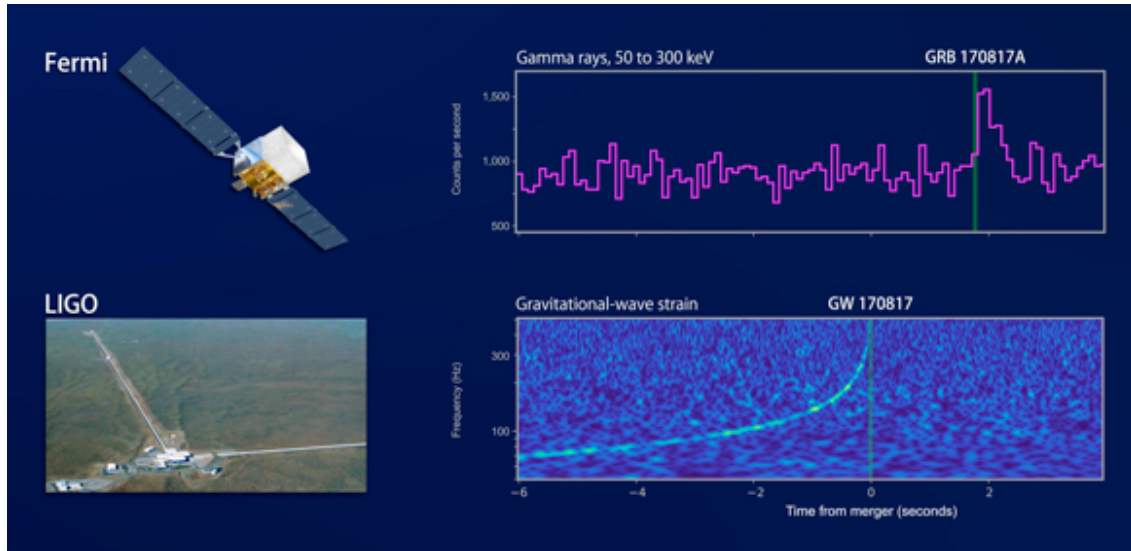
短伽马暴的喷流结构和光度函数

俞云伟 谈伟伟

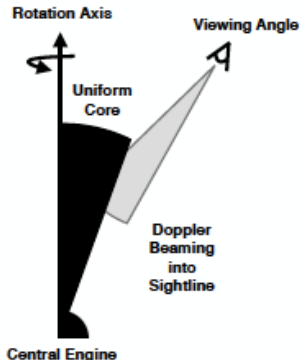
华中师范大学
湖北第二师范学院

2020年10月30日•北京•第二届GECAM研讨会

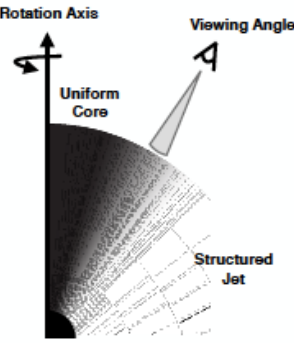
GW170817/GRB 170817A



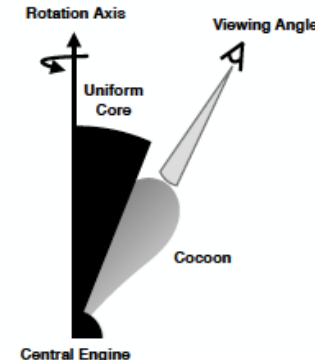
Scenario I: Uniform Top-hat Jet



Scenario II: Structured Jet

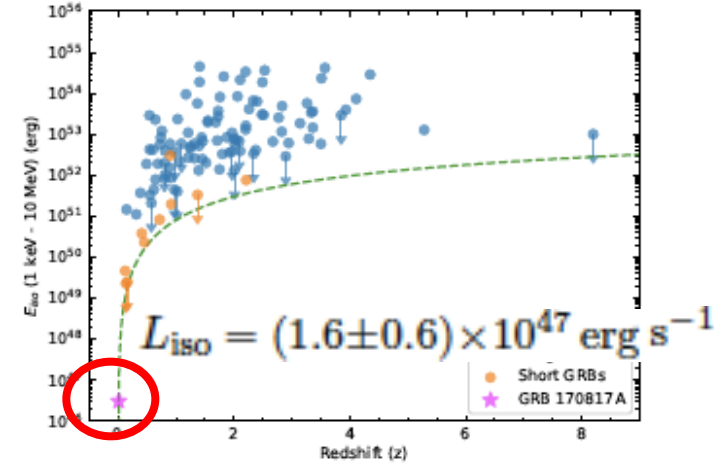
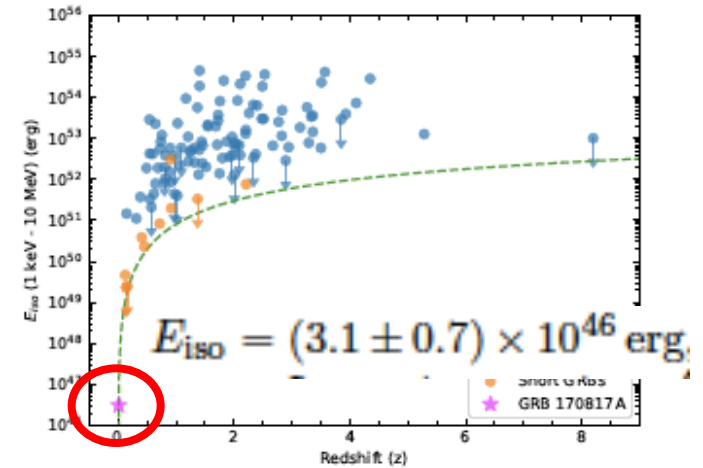


Scenario III: Uniform Jet + Cocoon



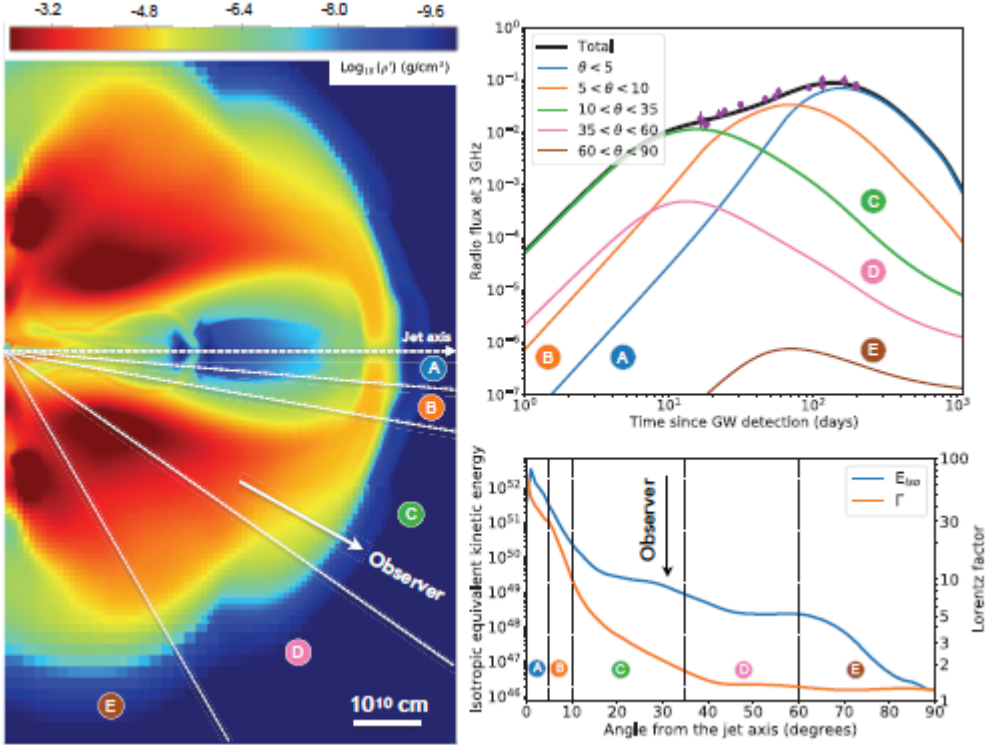
loka & Nakamura 1710.05905
Bromberg et al. 1710.05897

俞云伟, GECAM研讨会, 北京



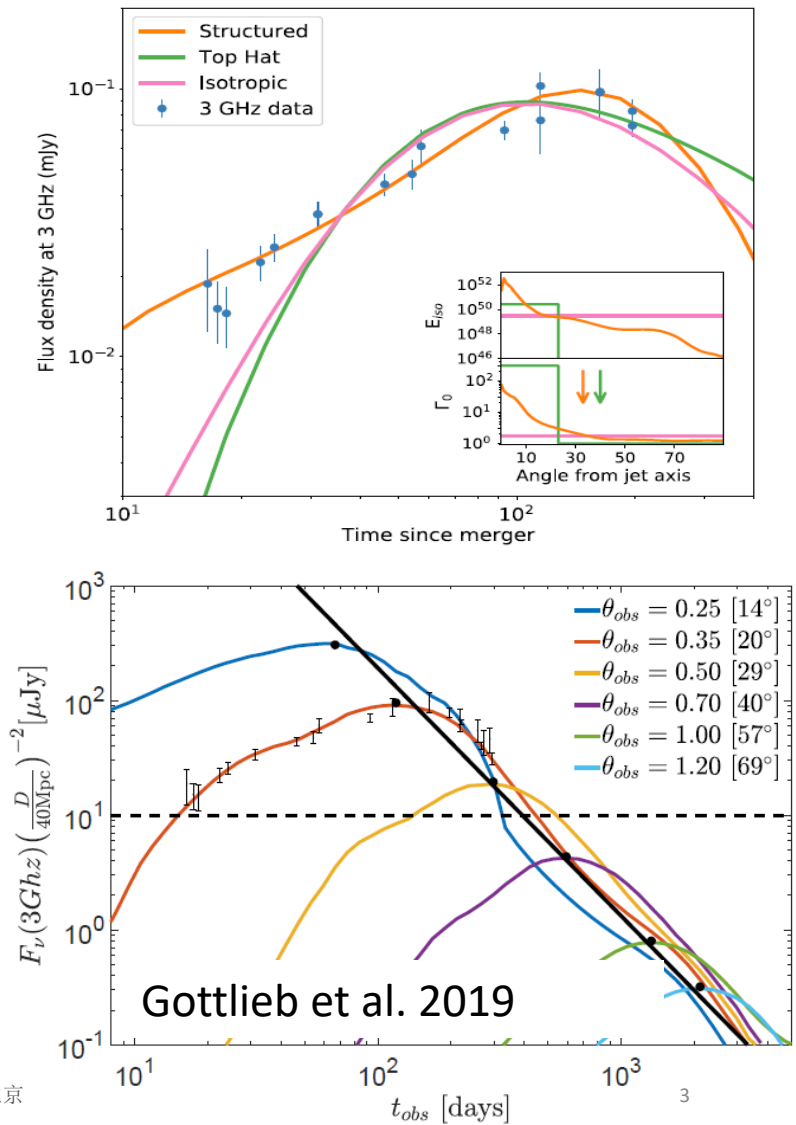
Abbott et al. 1710.05834

Jet structure and off-axis observational afterglows



Lazzati et al. 2018, PRL, 120: 241103

俞云伟, GECAM研讨会, 北京



Superluminal motion

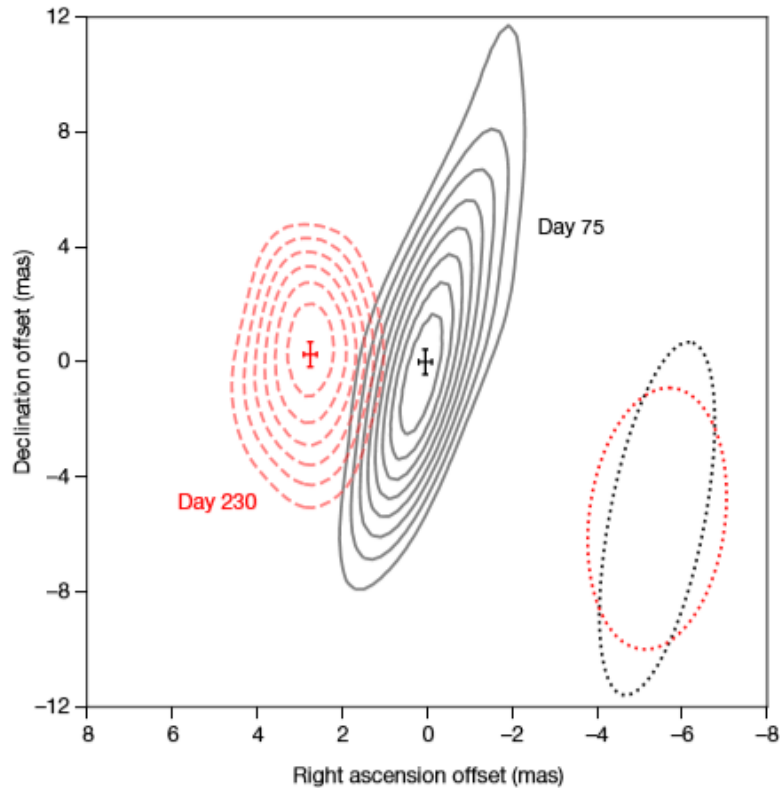
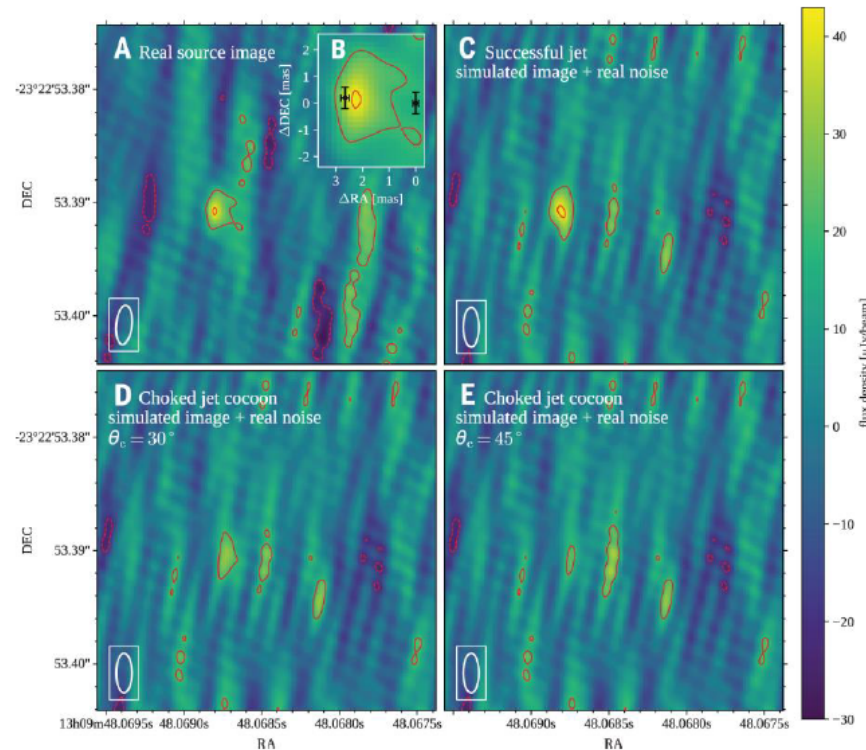


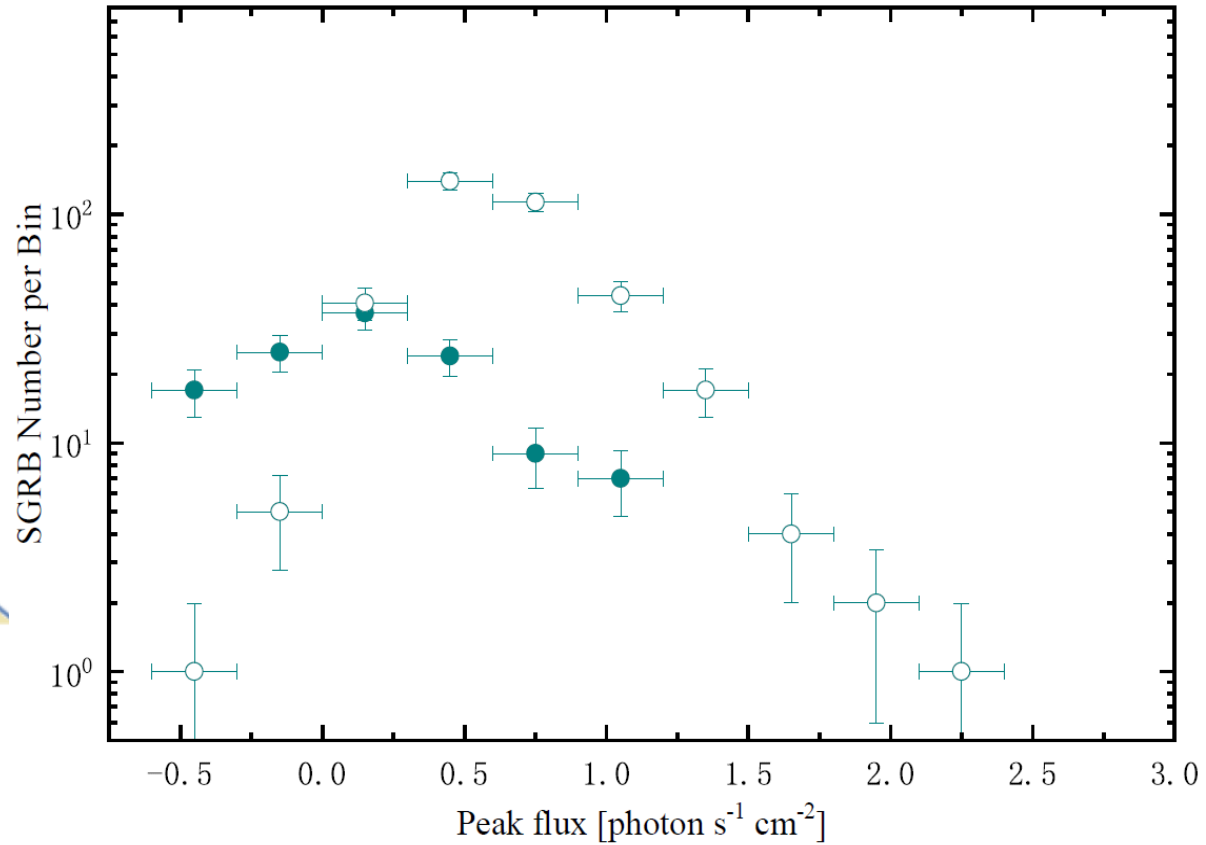
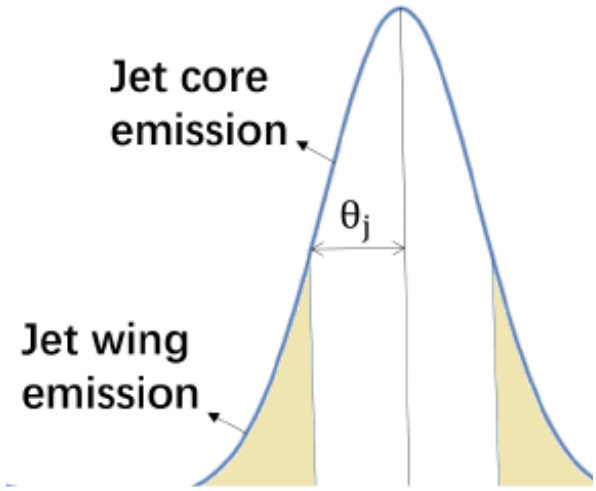
Fig. 1 | Proper motion of the radio counterpart of GW170817. The offset positions of the centroid (shown by 1σ error bars) and 3σ – 12σ contours of the radio source detected 75 days (black) and 230 days (red) after the merger event using VLBI at 4.5 GHz. The two VLBI epochs have

Mooley et al. 2018, Nature, 561: 355



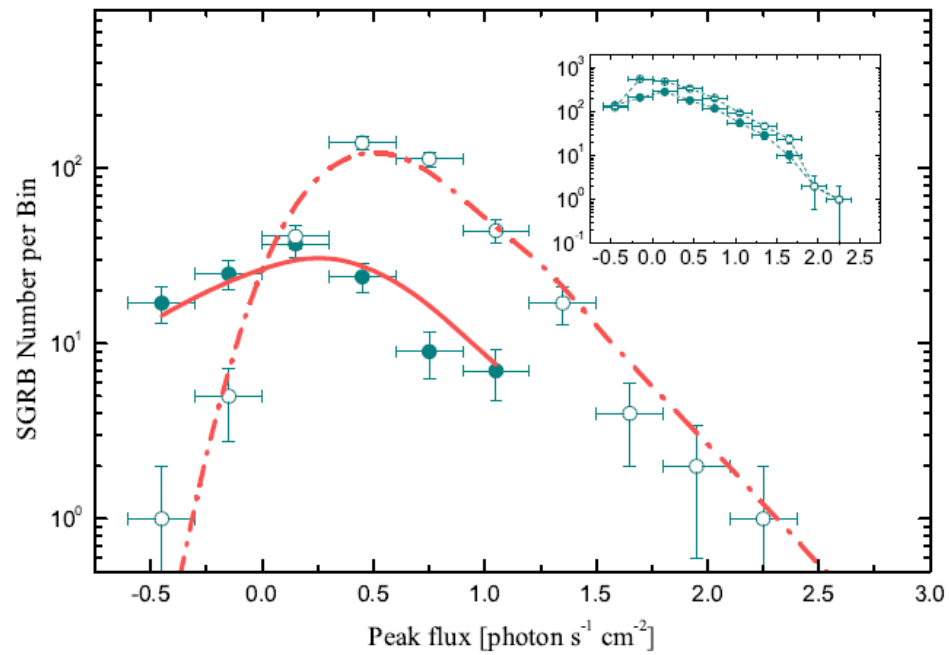
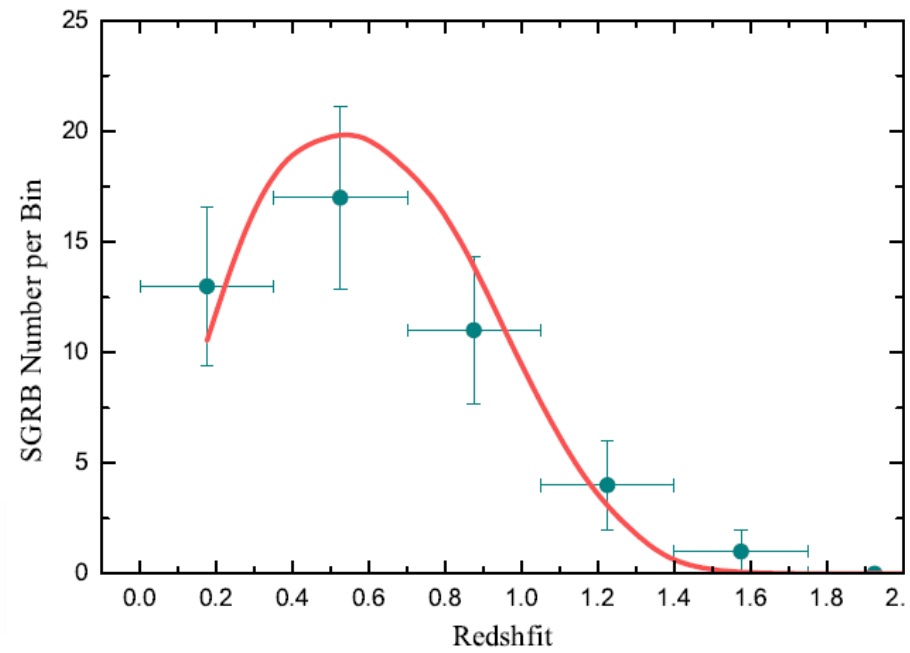
Ghirlanda et al. 2019, Science, 363: 968

Jet Structure



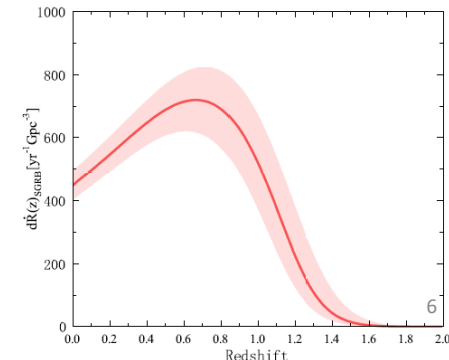
Flux and redshift distributions of cosmological SGRBs

Tan & Yu 2020, ApJ, 902, 83

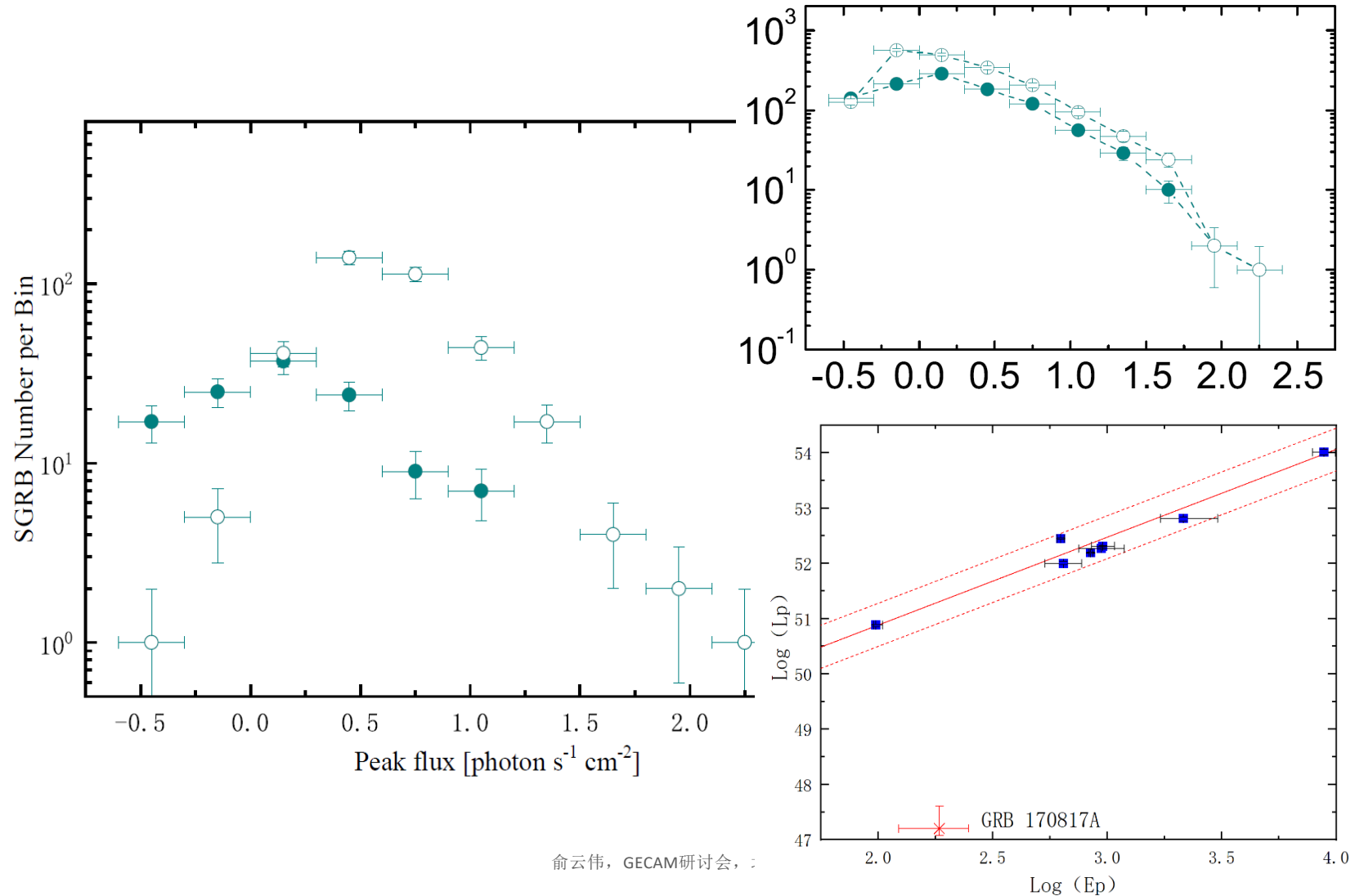


$$\begin{aligned}
 N(P_1, P_2) = & \frac{\Delta\Omega}{4\pi} T \int_0^{z_{\max}} \int_{P_1}^{P_2} \int_0^{\theta_{v,\max}} \\
 & \times \eta(P) \sin \theta_v d\theta_v dP \frac{dV(z)}{1 + \tilde{z}}, \quad (5)
 \end{aligned}$$

俞云伟, GECAM研讨会, 北京



Flux distribution and sensitivity



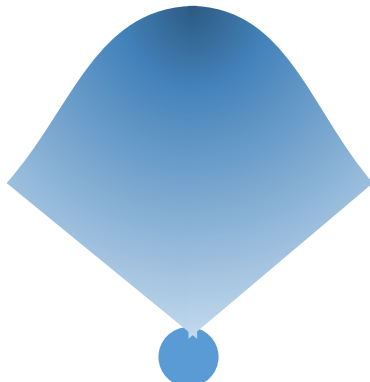
Jet structure and luminosity functions

Top-hat jet

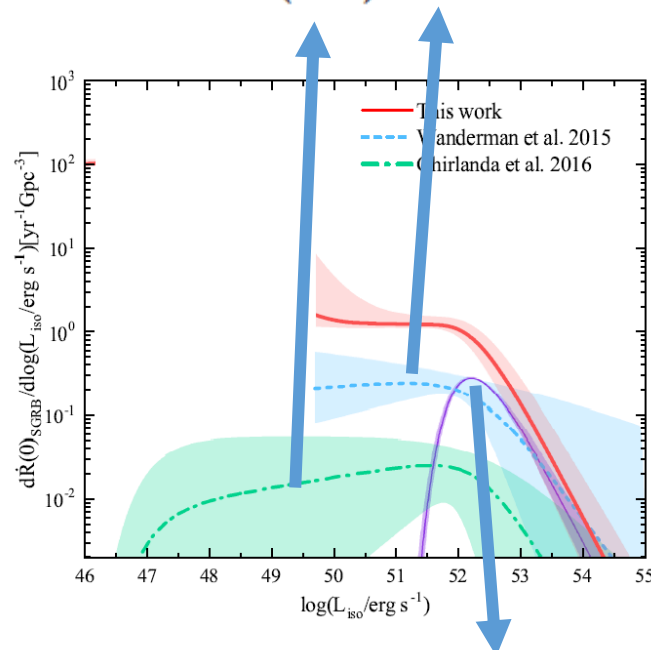


Gaussian jet

$$L_{\text{iso}}(\theta_v) = L_{\text{in,p}} \exp \left(-\frac{\theta_v^2}{2\theta_{\text{in}}^2} \right)$$



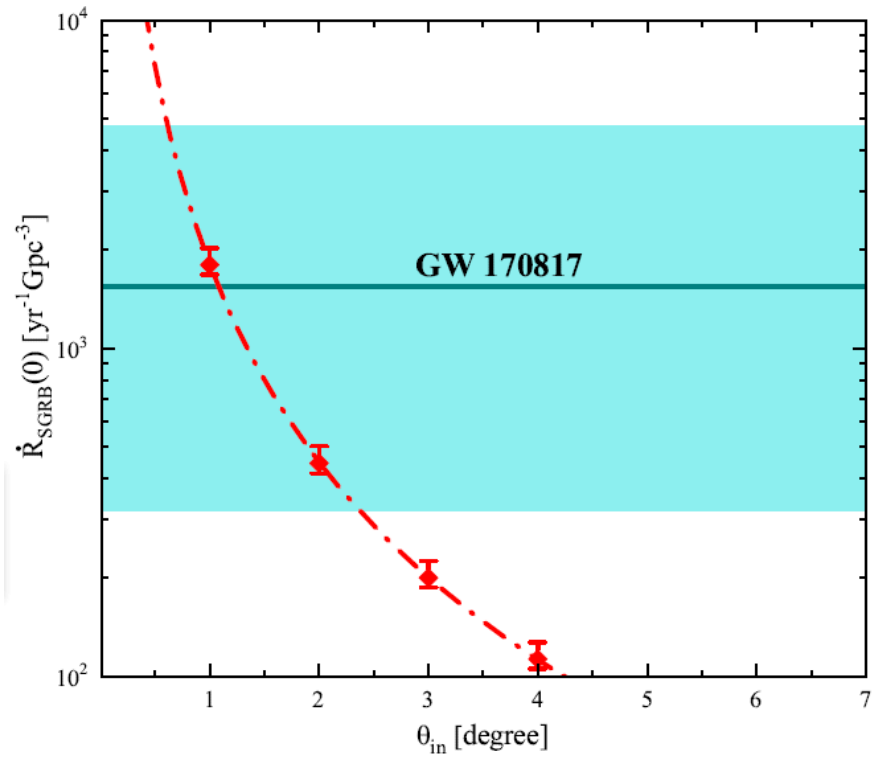
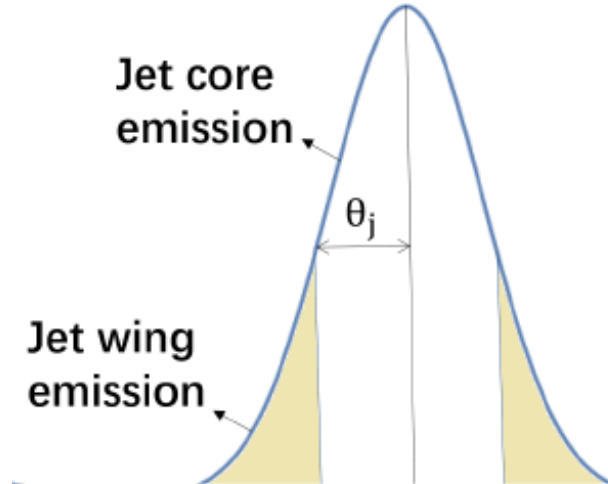
$$\Phi(L) \propto \begin{cases} \left(\frac{L}{L_b}\right)^{-\nu_1}, & L < L_b, \\ \left(\frac{L}{L_b}\right)^{-\nu_2}, & L \geq L_b. \end{cases}$$



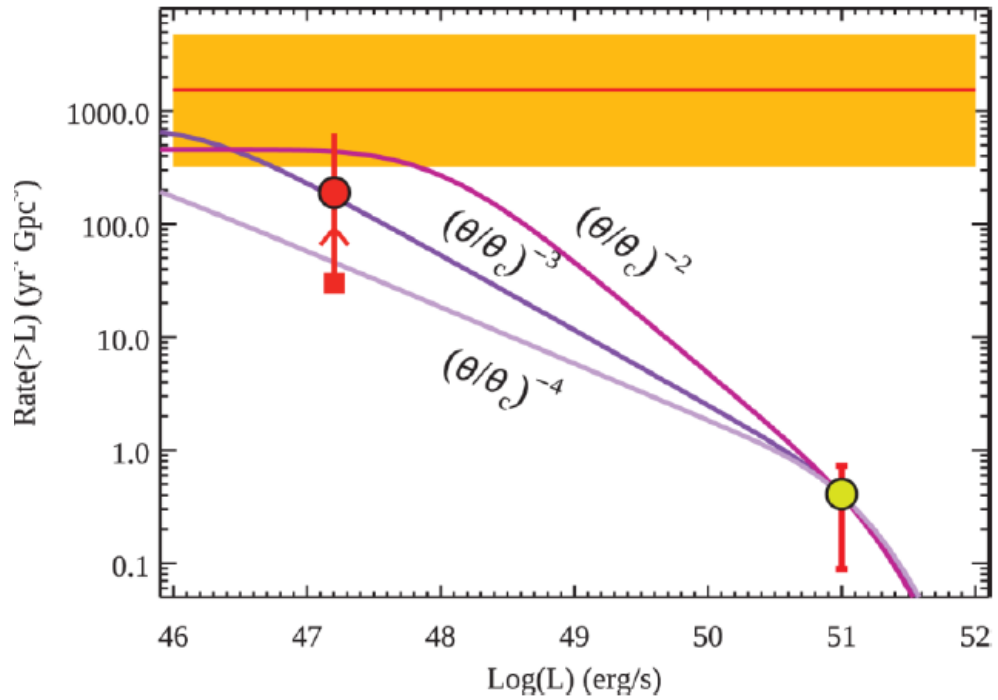
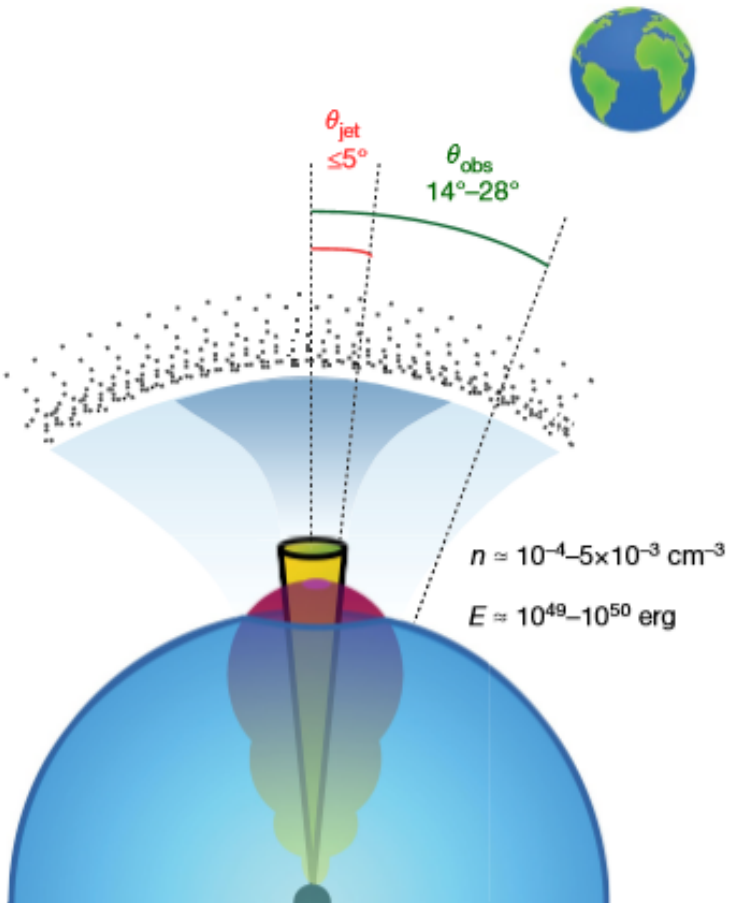
$$\Phi(L_c) = \Phi_* \left(\frac{L_c}{L_c^*} \right)^{-\gamma} \exp \left(-\frac{L_c^*}{L_c} \right)$$

Parameter constraints

Tan & Yu 2020, ApJ, 902, 83



Jet structure and GRB rate

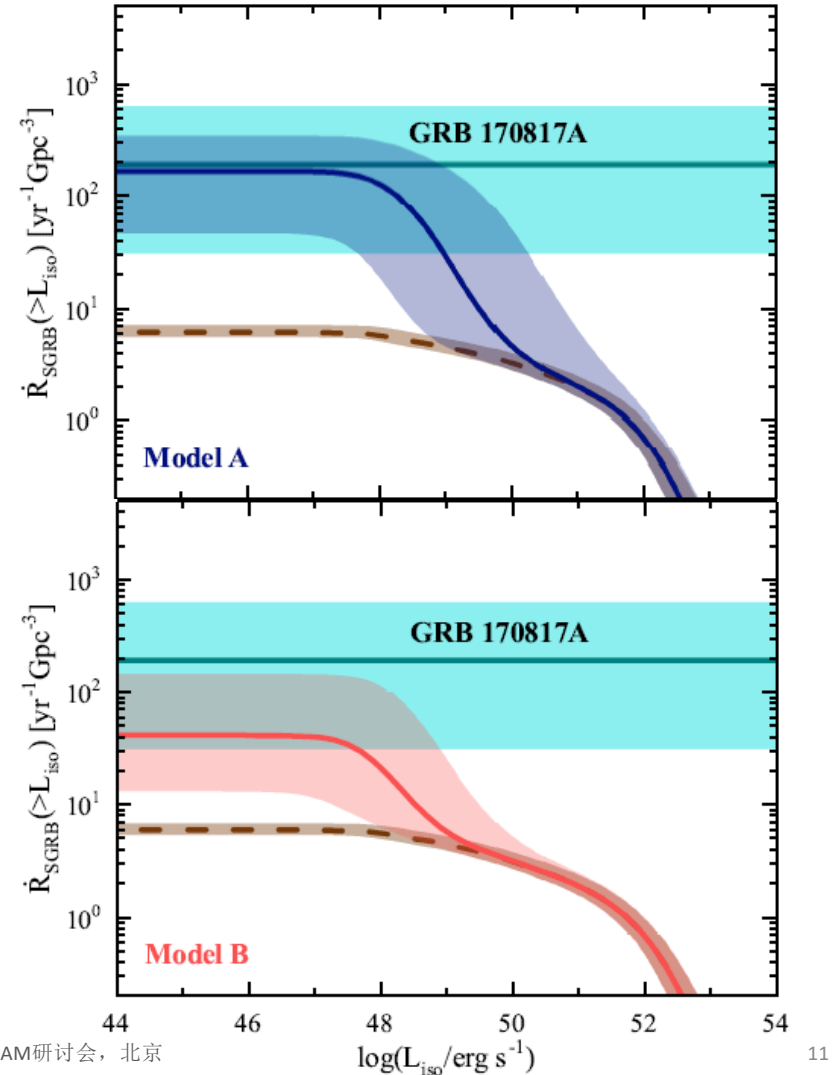
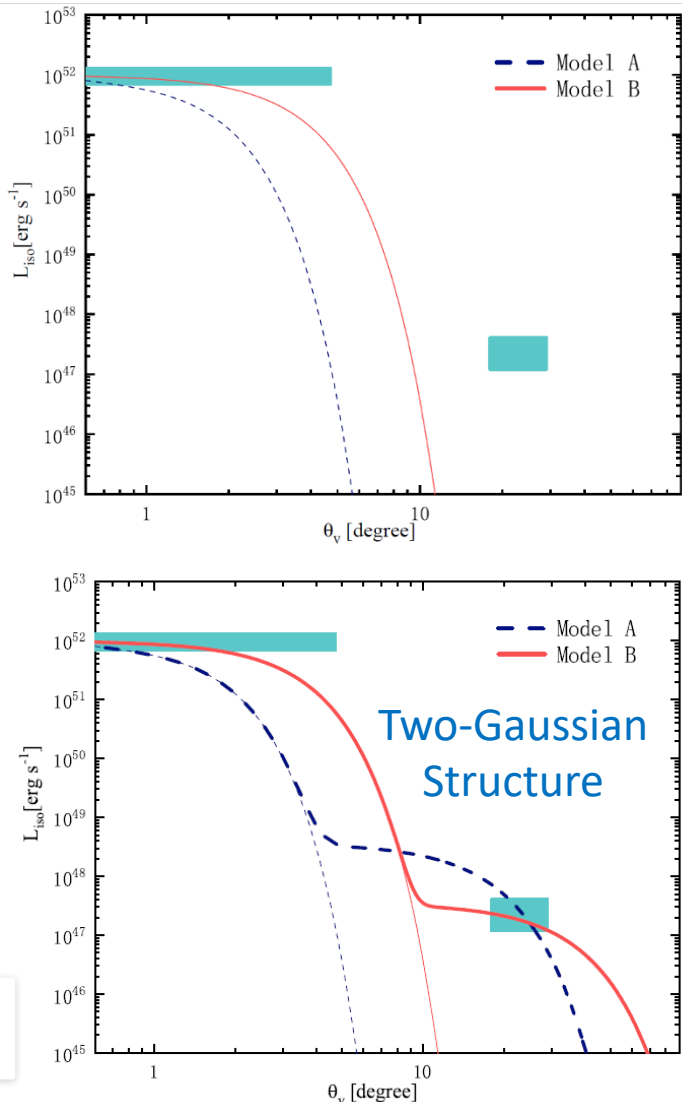


Ghirlanda et al. 2019, Science, 363: 968

Mooley et al. 2018, Nature, 561: 355

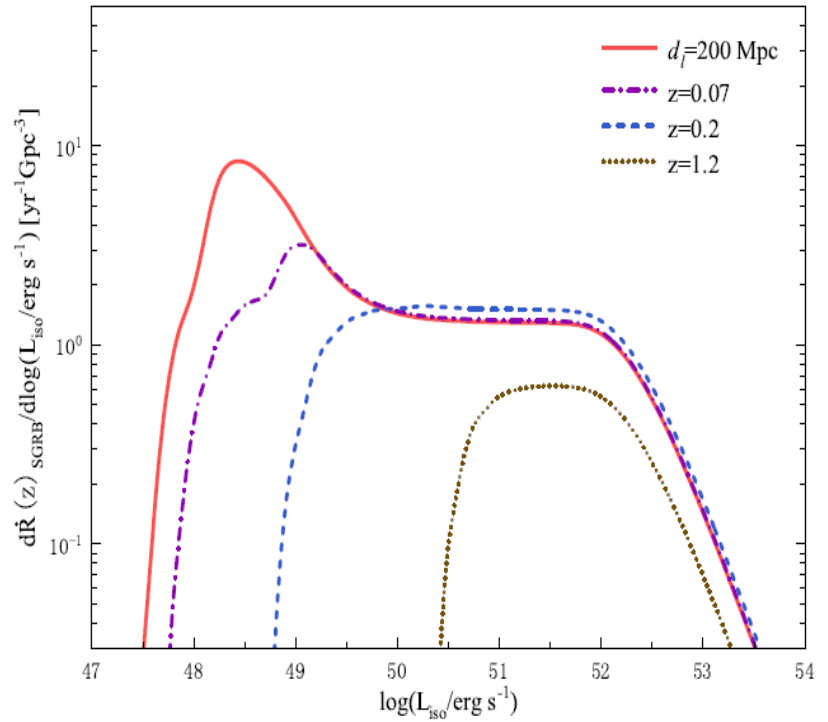
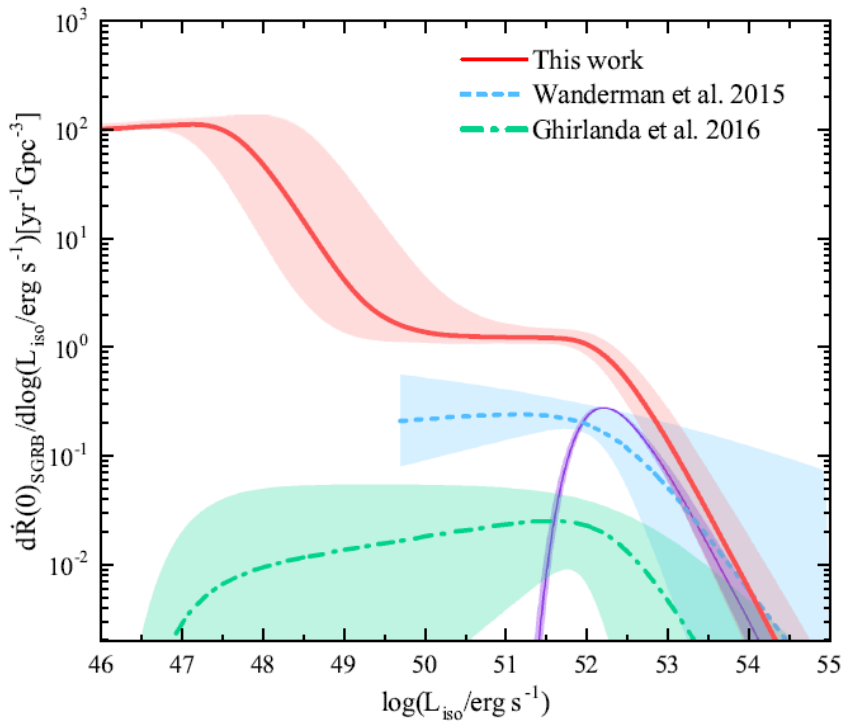
Parameter constraints

Tan & Yu 2020, ApJ, 902, 83



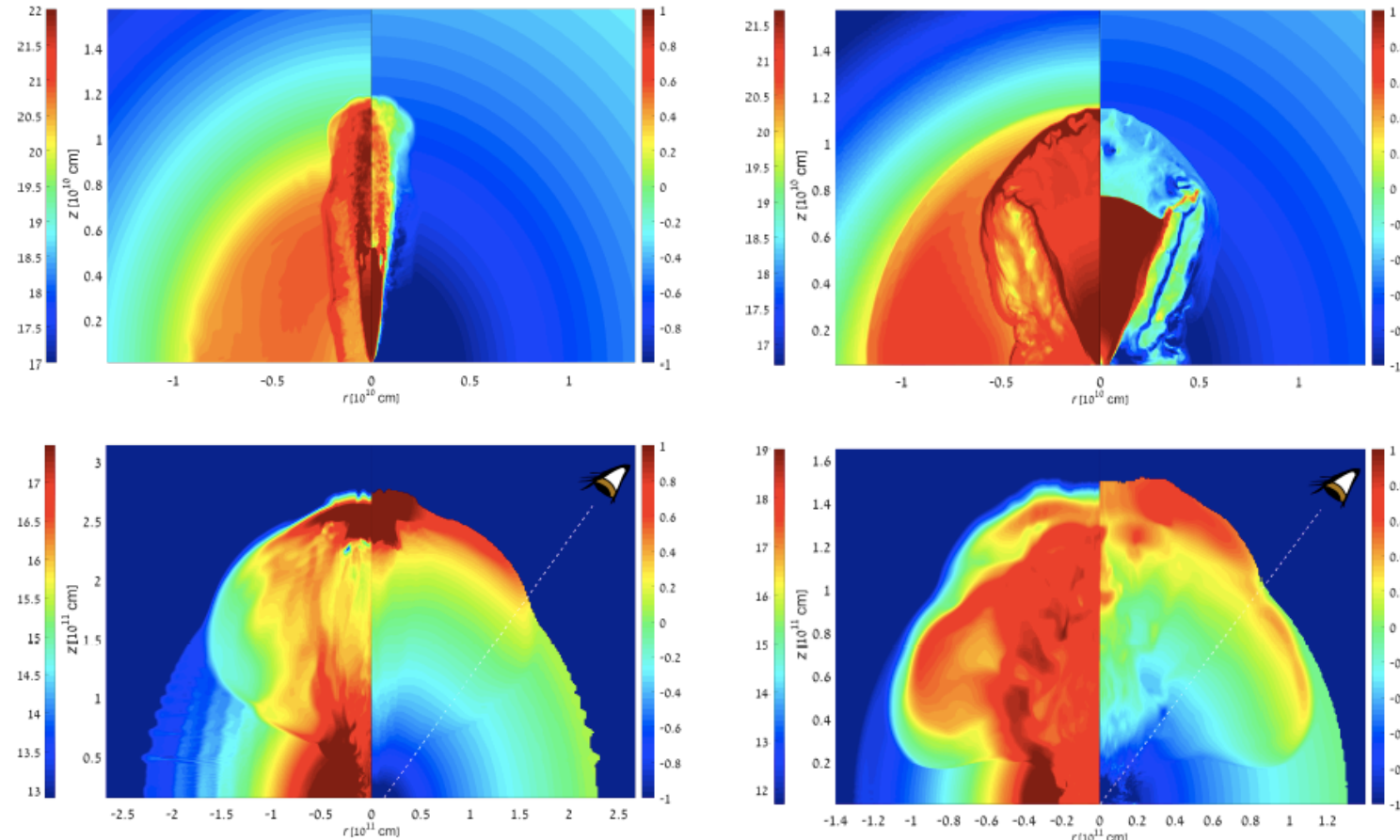
Luminosity functions

Tan & Yu 2020, ApJ, 902, 83



Jet breakout

Gottlieb et al. 2018, MNRAS, 479, 588



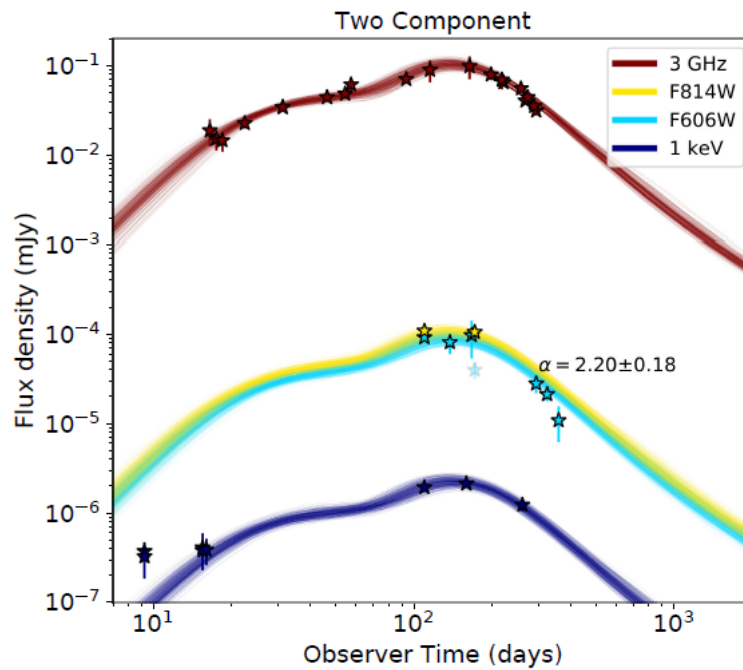
GECAM expectation

The detectable number per year of the GW-associated SGRBs for GECAM^[42].

Model	<100 Mpc	<200 Mpc	<300 Mpc
A	$0.9^{+0.6}_{-0.4}$	$7.9^{+4.7}_{-3.3}$	$20.9^{+15.4}_{-10.7}$
B	$0.4^{+0.4}_{-0.2}$	$3.3^{+2.8}_{-1.4}$	$9.3^{+9.1}_{-4.4}$

Two-component afterglow model

- The broadband afterglow is consistent with a structured outflow where an ultra-relativistic jet, with Lorentz factor, ~ 100 , forms a narrow core (5°) and is surrounded by a wider angular component that extends to 15° , which is itself relativistic ($\text{Gamma} > 5$).



Lamb et al., 2019, ApJ, 870, L15